Preventing corrosion by controlling cathodic reaction kinetics

Progress Report for Period: 1 SEP 2015 – 31 MAR 2016

John Keith
Department of Chemical & Petroleum Engineering
Swanson School of Engineering, University of Pittsburgh
804 Benedum Hall, 3700 O'Hara Street, Pittsburgh, PA 15261

***Acknowledgement/Disclaimer**: This work was sponsored by the Office of Naval Research, ONR, under grant/contract number N00173-15-1-G018. The views and conclusions contained herein are those of the authors and should not be interpreted as necessarily representing the official policies or endorsements, either expressed or implied, of the Office of Naval Research, the U.S. Navy or the U.S. government.*

Grant or Contract # N00173-15-1-G018
Date Prepared: 25 March 2016

Preventing corrosion by controlling cathodic reaction kinetics

Annual Summary Report: FY16

PI: John Keith, 412-624-7016, jakeith@pitt.edu

Section I: Project Summary

Overview of Project

Abstract:

Anti-corrosion coatings have been well studied as physical barriers for corrosible materials. However, less work has been done to understand how the electronic structure of an anti-corrosion coatings can be designed to limit the electrochemical reaction rates of processes that drive corrosion, e.g. the oxygen reduction reaction (ORR). To this end, we have used reactive forcefields and first principles quantum chemistry to model electrocatalysis on amorphous TiO_2 surfaces, an inexpensive and non-toxic coatings material. We report how surface models were obtained as well as feasible reaction pathways predicted using quantum chemistry. We then will show how metal dopants affect ORR reaction energies in order to better hinder ORR kinetics.

Objective:

The goal of this project is to determine the effect of dopant elements on the kinetics of oxygen reduction reaction catalyzed on titanium oxide in order to develop new approaches for controlling galvanic corrosion between fastener and structural aircraft alloys.

Introduction:

Galvanic corrosion generally refers to the corrosion damage that occurs when two dissimilar metals are electrically connected in the presence of a corrosive electrolyte. The corrosive electrolytes of interest to this program are aqueous in nature; that is, water acts as the solvent for various ionic and gaseous constituents. The ionic components of the electrolyte are commonly the result of various kinds of salt dissolution while the gaseous constituents diffuse in at the electrolyte-atmosphere boundary.

We can differentiate between bulk, *i.e.* high volume, and atmospheric, *i.e.* low volume, electrolytes in terms of the behavior of the ionic and gas components. In bulk electrolytes, the ionic concentration remains essentially unchanged regardless of the corrosion reactions occurring at the metal-electrolyte interface. The gas concentration, however, can be depleted at the metal-electrolyte interface because the electrolyte-atmosphere boundary is far from the reacting interface and diffusion transport across long distances is slow. In atmospheric electrolytes, the ionic population is considered finite and consumption of anions in reactions with metal cations can deplete the electrolyte. However, in the atmospheric electrolyte, the electrolyte-atmosphere boundary is close to the metal-electrolyte boundary so diffusion can, for example, resupply gas constituents consumed in reduction reactions.

Aqueous corrosion, both in bulk and atmospheric electrolytes, requires a coupled oxidation-reduction reaction, which may occur on neighboring regions on the same surface, an electronic conduction path, and the aforementioned water-based electrolyte for ionic transport between the reaction sites. In the case of galvanic corrosion, the sites for metal oxidation and oxygen reduction may be located on the different materials of the galvanic couple; thereby requiring the establishment of an electron conduction path that extends:

- From the oxidation site
- Through the bulk of the active metal or alloy
- Across the galvanic junction
- Through the bulk of the noble metal or alloy
- Across the noble metal oxide
- To the reduction reaction site

For this study, the protective oxide that forms on titanium is of interest because it is thermodynamically stable up to +1.5 V_{SHE} (+1.25 V_{SCE}) at pH 12 and, for the alkaline conditions expected to obtain when acting as the noble material in a galvanic couple, the electrochemical properties of the oxide dominate the metal's cathodic behavior. Within

an alkaline environment, we expect the following reduction reactions to be catalyzed on the oxide:

Table 1. Reactions, pH ranges, and potential ranges for the reduction reactions of interest for the electrolytes considered in this report.

Reaction	pH range	Potential range (V_{SHE})
$O_2 + 2H_2O + 4e^- \leftrightarrow 4OH^-$	7-14	+0.820 - +0.401
$2H_2O + 2e^- \leftrightarrow H_2 + 2OH^-$	7-14	-0.413 - -0.828

In the case of electrolytes that arise from atmospheric processes, the electrolyte is usually aqueous, thin, and may be localized on the surface, such as in the form of a droplet. Chemistries and pH in the electrolyte can vary greatly and the oxygen content of the electrolytes can be high. The discrete nature of the atmospheric electrolyte makes cathodic protection difficult and galvanic corrosion damage under these conditions can be difficult to detect. Figure 1 illustrates the components and processes of atmospheric galvanic corrosion.

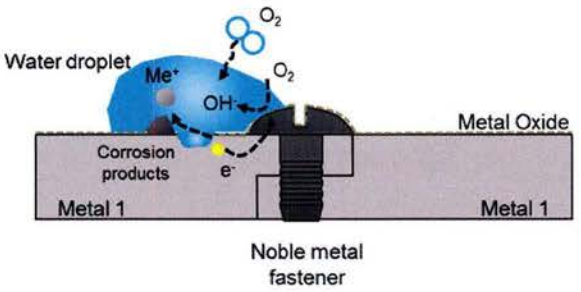

Figure 1. Illustration of galvanic corrosion in an atmospheric environment. The junction of the two plates of metal 1 with a noble metal fastener establishes the galvanic junction of dissimilar metals that can cause corrosion once a droplet of water forms on the surface. The high surface area-to-volume ratio of the droplet allows a high dissolved oxygen concentration to obtain even once the reduction reaction begins consuming oxygen. As a result, the electrolyte near the cathode becomes alkaline while the electrolyte near the anode becomes more acidic.

Many structural aircraft alloys, such as AA2024 and AA7075, have stable, corrosion resistant oxides, like those found on titanium. However, corrosion damage is frequently seen in areas that are near galvanic contacts between the aluminum alloys and fasteners made of titanium or steel alloys. The fastener material, which is more noble than the

aluminum, catalyzes a reduction reaction from species present in the electrolyte and drives oxidation in the structural alloy, despite the protective oxide.

The corrosion rate of the more active material is strongly influenced by, among other conditions such as the presence of aggressive anions, the amount of exposed surface area of the cathode and by the ability of the cathode to support a suitable reduction reaction, such as hydrogen evolution or oxygen reduction shown in Table 1. These two reduction reaction rates are themselves influenced by the concentrations of the reacting species in the electrolyte and by the catalytic properties of the material surface. In the case of the oxide on titanium, the oxide microstructure plays a critical role in determining the kinetics of the reduction reactions.

The approach taken in this report for modeling the oxygen reduction reaction on amorphous TiO_2 surfaces closely follows the approach of Nørskov et. al. (10.1021/jp047349j) by using electrochemical scaling relationships to determine the reaction overpotentials. For these calculations, the target calculation is an adsorbate binding energy for a molecule, M, bound to a surface defined as:

$$\Delta E = E([\text{Surface\_M}]) - E(\text{Surface}) - E(\text{M}) \qquad (6)$$

Where $E([\text{Surface\_M}])$, $E(\text{Surface})$, and $E(\text{M})$ represent the total energies of the surface model with the bound adsorbate, the clean surface, and the non-interacting adsorbate, respectively. Statistical thermodynamic approximations can be used to incorporate zero-point vibrational energies as well as enthalpic and entropic energy contributions to approximate Gibbs or Helmholtz free energies at finite temperatures as well. Our approach will utilize an amorphous TiO_2 surface utilizing periodic boundary conditions to simulate an extended TiO_2 surface.

Background:

The program was designed to address the following key tasks:

Task 1:

Generate an atomic scale amorphous TiO_2 surface that would be expected to form under long term exposure to maritime conditions

Task 2:

Predict ORR reaction energetics on inorganic oxide coating materials for improved understanding of fundamental reaction mechanisms that result in corrosion

Task 3:

Determine which dopant atoms are likely to cause a reduction in the cathodic kinetics. Theoretical frameworks have been calculated for hydrogen evolution reactions focused on hydrogen adsorption and oxygen reduction. Our theoretical approach is to extend these free energy based models to titanium based amorphous oxides with the focus on maximizing the band gap.

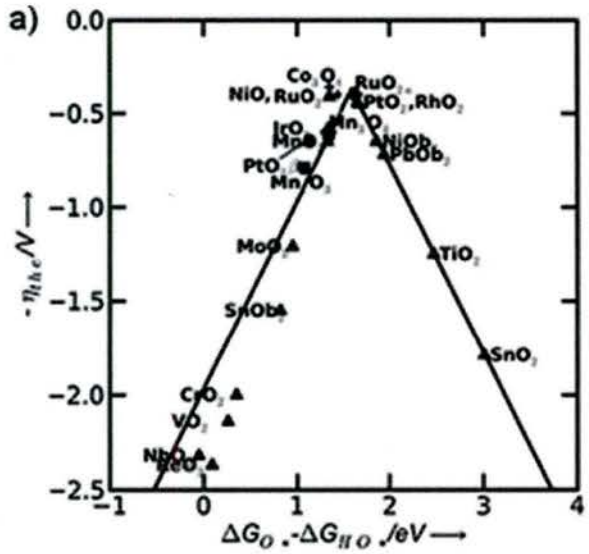

Figure 1: An example plot of overpotential vs. the binding energy for O and OH* for certain metal oxides. In this work, the approach is to start with oxide compositions near the base of the triangle.*

Activities and Accomplishments

Creating an Amorphous Surface with Computational Tools

We created a model amorphous TiO_2 surface by annealing a rutile 100 slab at 1000 K using ReaxFF as employed in LAMMPS. We used the force field created by Kim et. al. (DOI: 10.1021/la4006983) as it is specifically parameterized to model bulk TiO_2. We tested various slab sizes by varying the number of primitive unit cells along the x and y in the original rutile 100 slab. Figure 2 shows the Ti-Ti pair radial distribution function appears approximately converged by the 3x3 unit cell slab.

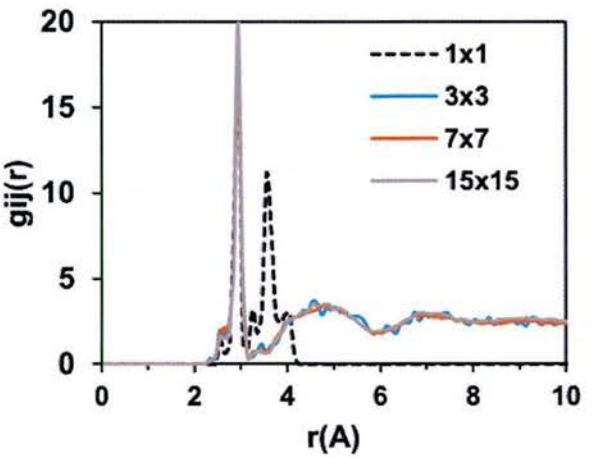

Figure 2. A comparison of the Ti-Ti pair radial distribution functions for various sizes of annealed TiO_2 slabs. The labels refer to the number of primitive rutile unit cells on each side of the slab prior to annealing.

We then relaxed the ReaxFF annealed structures using the Vienna *ab initio* simulation package (VASP). These calculations used the PBE exchange correlation functional, PAW psuedopotentials, energy cut offs of 450 eV, and a 2x2x1 kpoint grid. We found that these energy cutoffs and kpoint grids gave well converged oxygen vacancy formation energies. The VASP relaxed structure has Ti-Ti, Ti-O, and O-O radial distribution functions that match experimental RDF data more closely than the ReaxFF annealed structures (Figure 3). As such, this surface is a suitable model for a real amorphous TiO_2 surface.

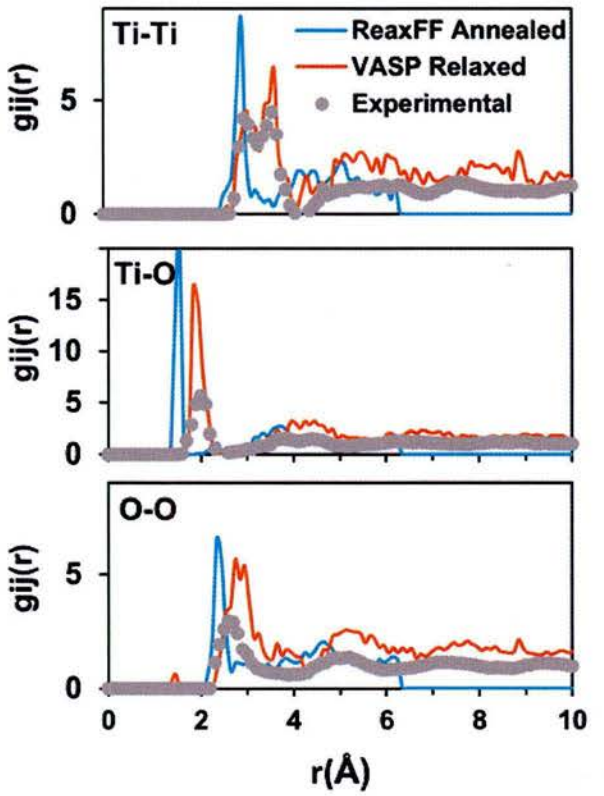

Figure 3. Comparing the Ti-Ti, Ti-O, and O-O radial distribution functions from ReaxFF annealed and VASP relaxed amorphous TiO_2 structures to experimental data (10.1016/S0022-3093(98)00418-9).

Modeled Two Possible ORR Mechanisms

We modeled two possible ORR mechanisms as proposed in Figure 4. The sites for these reactions can take place on the amorphous TiO_2 surface are highlighted in Figure 5.

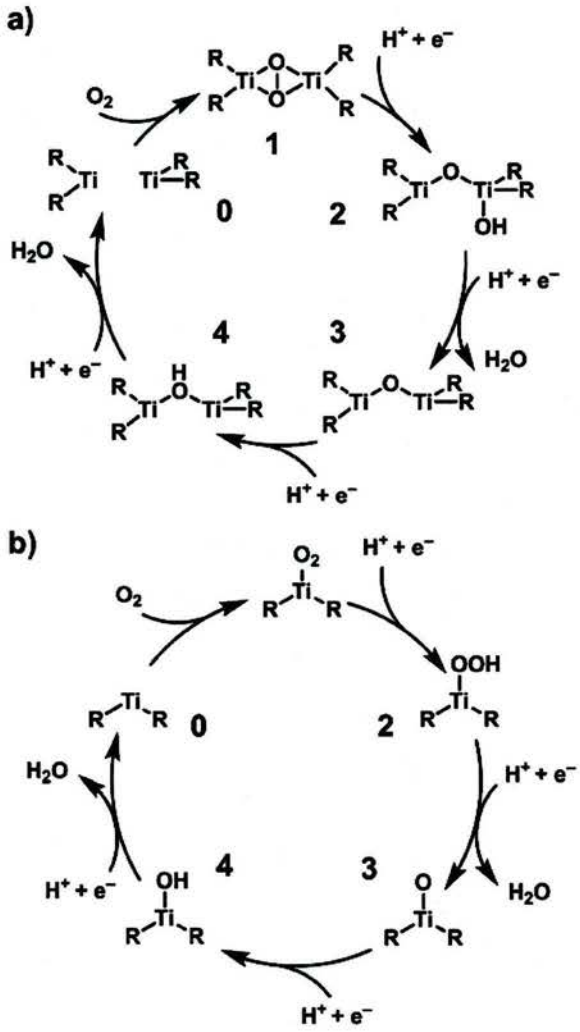

Figure 4. Proposed ORR mechanisms. A) Involves reaction intermediates adsorbed in a surface O vacancy, b) involves reaction intermediates adsorbed to the top of a surface Ti site.

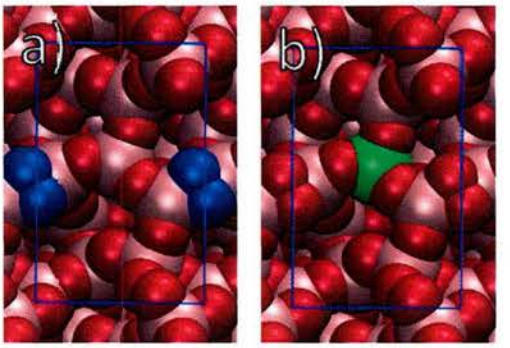

Figure 5. The amorphous TiO_2 surface used. A) Highlights an O_2 adsorbed into a surface O vacancy (Figure 4a, structure 1), B) highlights a surface Ti site for mechanism b (Figure 4b, structure 0).

Findings and Conclusions

Figure 6 shows that the first three steps in the vacancy reaction mechanism (Figure 4a) are ~7 eV downhill in energy, but there is a significant barrier (>1.5 eV) to regenerate the vacancy site. This suggests that the vacancy sites are quickly replenished with oxygen atoms, but the vacancy sites are not easily regenerated. This barrier to regenerate the active site suggests that this is not the primary mechanism for ORR on amorphous TiO_2 surfaces.

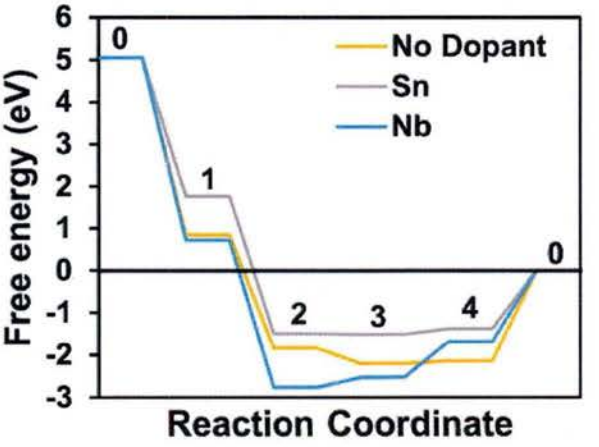

Figure 6. The relative energetics for the vacancy mechanism in Figure 4a with an applied potential of 0 V vs RHE.

The surface ORR mechanism (Figure 4b) is more feasible and our calculations predict that ORR on amorphous TiO_2 occurs with an overpotential of ~0.45 V vs RHE. Figure 7 shows that the energetics of the surface ORR intermediates can vary by up to ~1 eV on different surface Ti sites. Site 4 has the lowest over potential (0.45 eV) of the sites that we identified and is therefore considered as the most reactive site in later calculations.

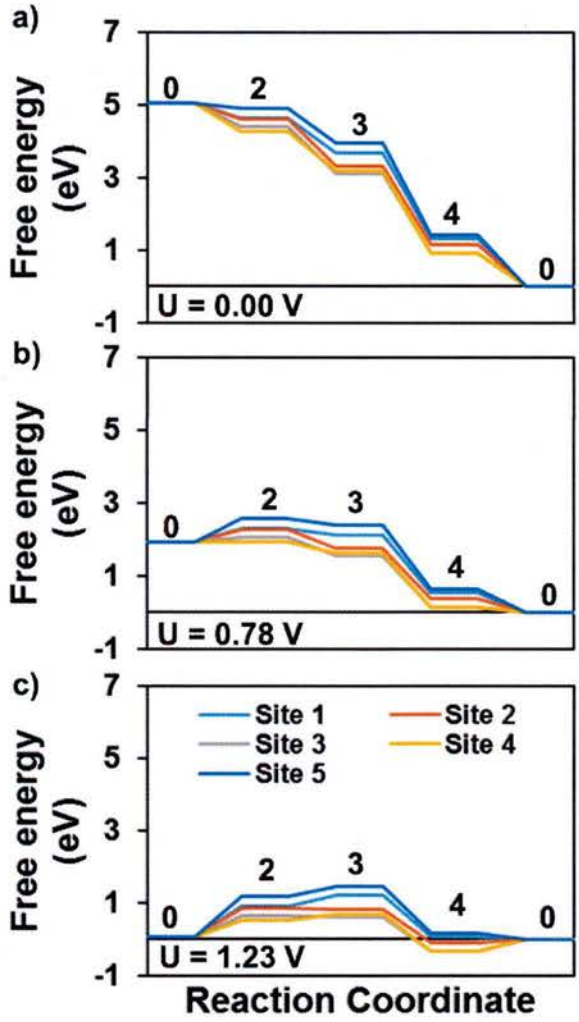

Figure 7. Relative energetics for the surface ORR mechanism shown in Figure 4b. The sites are labeled according to the proposed mechanism in Figure 4b. The relative energetics are displayed at a) 0 V vs RHE, b) 0.78 V vs RHE, and c) 1.23 V vs RHE. The

reaction over potential dictated by the most energetically uphill reaction step at U = 1.23 V vs RHE.

We studied *OOH, *O, *OH adsorbed to the surface for a variety of metal dopants on site 4. To determine the impact of dopants, the Ti atom at site 4 was replaced with the dopant of interest, and we relaxed the structure of each ORR intermediate on the resulting surface. This assumes both that the dopant will be most effective if the intermediates directly adsorb to it and that limiting the reaction at the most reactive site will limit ORR activity. Plotting the *OOH and *OH energies (Figure 8) shows that there is a scaling relationship between these two intermediates that can be used to create a volcano plot.

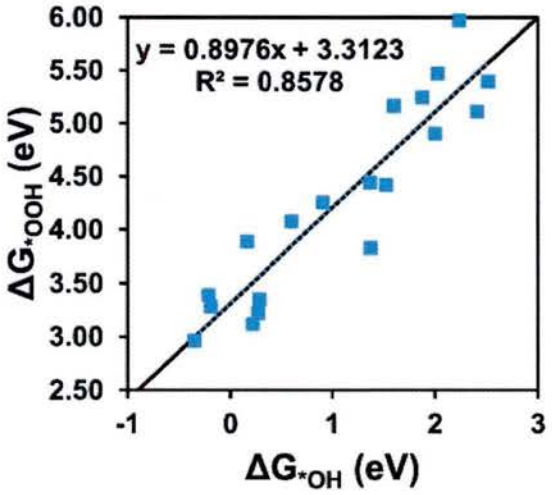

Figure 8. The scaling relationship between the energy of *OOH and *OH bound to the surface for all of the dopants tested. This relationship is used to create the volcano plot in Figure 9 and Figure 11.

We considered dopants at site 4 (the most reactive site) and several dopants on site 5 (the originally least reactive site). Several key insights can be learned from comparing the dopant effects at these two reaction sites. First, dopants that destabilize the ORR intermediates on the amorphous TiO_2 surfaces will hinder ORR activity on any site. When we compare site 4 and 5, we can clearly see that the dopants that destabilize the intermediate (increasing the *OH energy) increase the reaction overpotential (and decrease reactivity) for both sites.

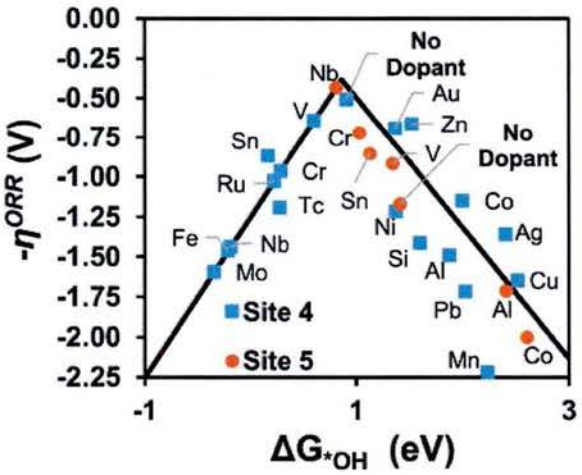

Figure 9. Compares the negative of the reaction overpotential against the *OH energy. This produces a volcano plot for ORR on a doped amorphous TiO_2 surface. Site 4 is the most active site without metal dopants. Site 5 shows how the reaction overpotential varies with reaction site.

The effect of dopants that stabilize the ORR intermediates are not as easily determined. Considering other reaction sites shows that these dopants could result in a smaller overpotential and increased ORR activity. In the case of niobium, the Nb doped site 5 has a lower overpotential than undoped site 4. This is consistent with other reports that Nb doped TiO_2 has increased ORR activity. This effect is illustrated in Figure 10 by comparing the relative energetics at site 4 and 5 at an applied potential = 1.23 V vs RHE.

Figure 10 shows that dopants may not have a uniform effect on the intermediate energies. For example:

1. Al and Co destabilize *OOH and *OH. The resulting uphill reaction to reach these states for dopants with similar behavior will increase the overpotential of any considered reaction site.
2. Sn stabilizes *OOH/*OH and destabilizes *O. The resulting uphill reaction to reach *O will increase the overpotential on any reaction site for dopants with similar effects.
3. Nb stabilizes all the intermediates, but results in similar *O/*OH energies at the equilibrium potential. This creates an energy well for site 4 (Figure 10a) and results in a larger overpotential. But considering these dopants at site 5 (Figure 10b) shows that the dopant stabilizes the intermediates with the effect of decreasing the reaction overpotential. This suggests the variety of available

surface sites could produce a smaller overpotential for that dopants that determine their overpotential from the *OH to * reaction step.

4. Cr stabilizes all of the intermediates, but results in a *O with a significantly lower energy than *OH at the equilibrium potential. Dopants with similar effects to Cr are limited by the *O to *OH step, which does not appear to significantly vary across the considered reaction sites.

As a result, dopants that determine their reaction overpotential from the *OH to * step might result in an increase in ORR activity. The overpotential for dopants similar to Sn and Cr are determined by intermediates whose relative energy remains relatively constant with different reaction sites. This produces overpotentials that may not scale well on volcano plots that use the energy of *OOH/*OH as a descriptor.

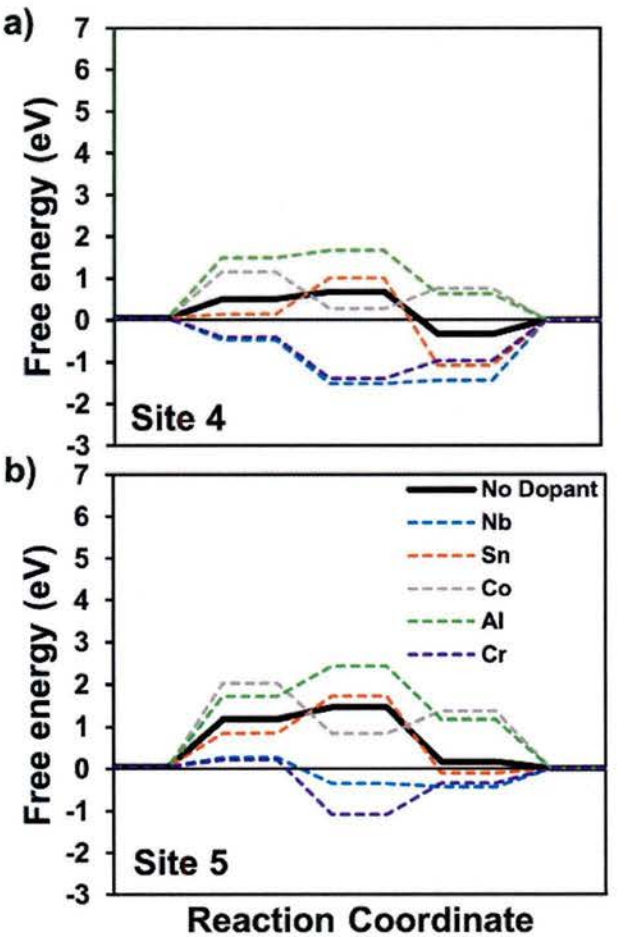

Figure 10. Highlighting how dopants influence the thermodynamic energies at different binding sites at an applied potential = 1.23 V vs RHE. A) the site with the lowest identified reaction overpotential, b) the site with the highest identified overpotential.

The revised volcano plot in Figure 11 color codes these different dopant types. While the blue dopants effect may vary at different surface sites, the dopants that fall on the right slope should always hinder the reaction kinetics by destabilizing intermediates. Blue dopants on the left slope have the potential to increase reaction kinetics at certain surface sites as we previously showed with Nb. The red and purple dopants (Sn, Ni, V, Cr, Tc, Mo) should prompt a decrease in ORR activity at all surface sites because their overpotentials result from reactions steps whose energetics do not significantly vary with surface site.

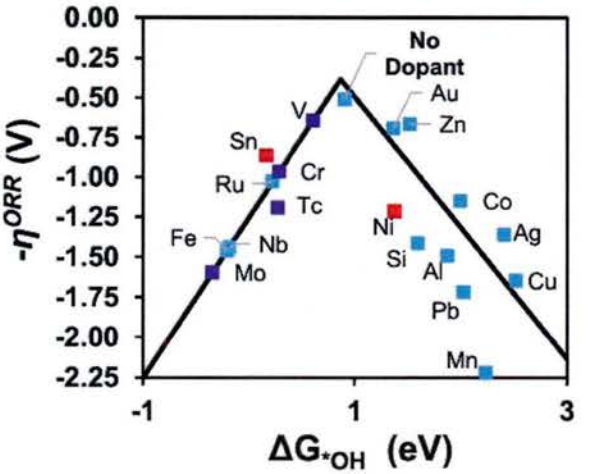

Figure 11. The volcano plot resulting from plotting the negative of the reaction over potential against the *OH energy. The over potential for blue data points is dictated by destabilization/stabilization of *OOH/*OH Red data points correspond to dopants that increase the reaction overpotential by destabilizing the *O intermediate opposed to those that stabilize/destabilize *OOH/*OH. Purple data points correspond to dopants that cause an uphill *O to *OH reaction step.

Our prediction that Co, Sn, and Cr will have lower ORR activity than pure TiO_2 is consistent with the previous experimental report. Fine tuning our model to predict the correct relative magnitude of the decrease in ORR activity would require future work to analyze the impact of each elementary reaction step on the overall ORR process. Currently, we predict that any dopant that destabilizes the intermediates ($\Delta G_{*OH} > 1$ eV) will hinder ORR kinetics. While we also believe that certain dopants with $\Delta G_{*OH} < 1$ eV can reduce ORR reaction rates (V, Sn, Cr, Mo) more work is required to completely understand the impact of these dopants.

Plans and Upcoming Events

The next steps in this research program are:

- Meeting with NRL collaborators in Spring 2016
- Presentation of results at the Fall ACS meeting in Philadelphia
- Submit first journal publication (Summer 2016)

Recommendations for Future Work:

1. Incorporating the effects of explicit surface-solvent interactions is missing from this work. While these effects could be accounted for by including corrections from continuum solvation models, explicitly including these interactions would increase the accuracy of our predictions.
2. Studying the impact of each elementary reaction step on the overall ORR process with a microkinetic model that combines experimental data and computationally studying the dopants at different surface sites.

Transitions and Impacts

Personnel

Principal investigator: John A. Keith

Team Members: Mitchell C. Groenenboom, Karthikeyan Saravanan, Yasemin Basdogan

Publications

Publications resulting from this project:

Journal Articles

Groenenboom, M. C.; Saravanan, K. Keith, J. A. "Controlling oxygen reduction reaction kinetics on anti-corrosion coatings via doping" *in preparation.*

Conference Papers

N/A

Other Publications

N/A

Recommended Reading and References

B. Zaid, D. Saidi, A. Benzaid, and S. Hadji, Corrosion Science, vol. 50, pp. 1841-1847, 2008.

M. Pourbaix, Atlas of Electrochemical Equilibria in Aqueous Solutions. Houston: National Associaton of Corrosion Engineers, 1974.

B. Wang, Journal of Power Sources, vol. 152, pp. 1-15, 2005.

D. Walther, M. Ruben, and S. Rau, Coordination Chemsitry Reviews, vol. 182, pp. 67-100, 1999.

C. Liu, T. R. Cundari, and A. K. Wilson, Inorganic Chemistry, vol. 50, pp. 8782-8789, 2011.

L. Y. Isseroff and E. A. Carter, Chemistry of Materials, vol. 25, pp. 253-265, 2013.

S. Maldonado and K. J. Stevenson, Journal of Physical Chemistry B, vol. 109, pp. 4707-4716, 2005.

K. K. Chin, Journal of Applied Physics, vol. 111, pp. 104509-104518, 2012.

J. Greeley, J. K. Norskov, and M. Mavrikakis, Annual Review of Physical Chemistry, vol. 53, pp. 319-348, 2002.

Y. Xu and M. Mavrikakis, Journal of Physical Chemistry B, vol. 107, pp. 9298-9307, 2003.

I. C. Man et al., ChemCatChem, vol. 3, pp. 1159-1165, 2011.

V. May and O. Kuhn, Charge and Energy Transfer Dynamics in Molecular Systems.: Wiley-Vch, 2004.

Cumulative List of Journal Articles, Conference Papers and Other Publications

N/A

Point of Contact in Navy

Steven Policastro.

Acknowledgement/Disclaimer

This work was sponsored by the Office of Naval Research, ONR, under grant/contract number N00173-15-1-G018. The views and conclusions contained herein are those of the authors and should not be interpreted as necessarily representing the official policies or endorsements, either expressed or implied, of the Office of Naval Research, the U.S. Navy or the U.S. government.

REPORT DOCUMENTATION PAGE

Form Approved
OMB No. 0704-0188

1. REPORT DATE *(DD-MM-YYYY)*	2. REPORT TYPE	3. DATES COVERED *(From - To)*
08/04/2016	Final Technical	09/23/15 - 04/22/16

4. TITLE AND SUBTITLE
Preventing Corrosion by Controlling Cathodic Reaction Kinetics

5a. CONTRACT NUMBER

5b. GRANT NUMBER
N00173-15-1-G018

5c. PROGRAM ELEMENT NUMBER

6. AUTHOR(S)
Keith, John, A

5d. PROJECT NUMBER

5e. TASK NUMBER

5f. WORK UNIT NUMBER

7. PERFORMING ORGANIZATION NAME(S) AND ADDRESS(ES)
University of Pittsburgh
Office of Research
123 University Place
Pittsburgh, PA 15213-2303

8. PERFORMING ORGANIZATION REPORT NUMBER
411367 - Final

9. SPONSORING/MONITORING AGENCY NAME(S) AND ADDRESS(ES)
Naval Research Laboratory
4555 Overlook Ave. SW
Washington, DC 20375

10. SPONSOR/MONITOR'S ACRONYM(S)
NRL

11. SPONSOR/MONITOR'S REPORT NUMBER(S)

12. DISTRIBUTION/AVAILABILITY STATEMENT
Approved for Public Release; Distribution is Unlimited

13. SUPPLEMENTARY NOTES

14. ABSTRACT
Our work focuses on understanding how the electronic structure of an anti-corrosion coatings can be designed to limit the electrochemical reaction rates of processes that drive corrosion, e.g. the oxygen reduction reaction (ORR). We have used reactive forcefields and first principles quantum chemistry to model electrocatalysis on amorphous TiO2 surfaces. We report how surface models were obtained as well as feasible reaction pathways predicted using quantum chemistry. We then will show how metal dopants affect ORR reaction energies in order to better hinder ORR kinetics.

15. SUBJECT TERMS
anti-corrosion coatings, oxygen reduction reaction, density functional theory, reactive forcefields

16. SECURITY CLASSIFICATION OF:			17. LIMITATION OF ABSTRACT	18. NUMBER OF PAGES	19a. NAME OF RESPONSIBLE PERSON
a. REPORT	b. ABSTRACT	c. THIS PAGE			Dr. John A. Keith
U	U	U	UU		19b. TELEPHONE NUMBER *(Include area code)* 412-624-7016